RESEARCH PAPER

Distribution and Visualisation of Chlorhexidine Within the Skin Using ToF-SIMS: A Potential Platform for the Design of More Efficacious Skin Antiseptic Formulations

Amy M. Judd • David J. Scurr • Jon R. Heylings • Ka-Wai Wan • Gary P. Moss

ABSTRACT

Purpose In order to increase the efficacy of a topically applied antimicrobial compound the permeation profile, localisation and mechanism of action within the skin must first be investigated.
Methods Time-of-flight secondary ion mass spectrometry (ToF-SIMS) was used to visualise the distribution of a conventional antimicrobial compound, chlorhexidine digluconate, within porcine skin without the need for laborious preparation, radio-labels or fluorescent tags.
Results High mass resolution and high spatial resolution mass spectra and chemical images were achieved when analysing chlorhexidine digluconate treated cryo-sectioned porcine skin sections by ToF-SIMS. The distribution of chlorhexidine digluconate was mapped throughout the skin sections and our studies indicate that the compound appears to be localised within the *stratum corneum*. In parallel, tape strips taken from chlorhexidine digluconate treated porcine skin were analysed by ToF-SIMS to support the distribution profile obtained from the skin sections.

A. M. Judd (✉) • G. P. Moss
School of Pharmacy, Keele University, Keele
Staffordshire ST5 5BG, UK
e-mail: a.m.judd@keele.ac.uk

D. J. Scurr
School of Pharmacy, University of Nottingham, Nottingham, UK

J. R. Heylings
Dermal Technology Laboratory Ltd.
MedIC4, Keele University Science Park, Keele, Staffordshire, UK

K.-W. Wan
School of Pharmacy and Biomedical Sciences
University of Central Lancashire, Preston, UK

Conclusions ToF-SIMS can act as a powerful complementary technique to map the distribution of topically applied compounds within the skin.

INTRODUCTION

Skin and soft-tissue infections (SSTIs) can range from non-complex cellulitis through to life threatening deep-seated subcutaneous tissue infections. Staphylococcal resistance is a clinical challenge and also for the management of skin and soft-tissue infections [1]. Skin infections resulting in cases of Methicillin-resistant *Staphylococcus aureus* (MRSA) bacteraemia increased from 25% to 32% between October and December 2011 [2]. Effective skin antisepsis has become the strategy of choice to reduce the number of complicated health care acquired infections (HCAIs), and it is also a key strategy in reducing the transmission of pathogens.

A potentially pathogenic microbiological flora inhabits the skin including the reduced environments of the skin's structures such as hair follicles, sebaceous glands, apocrine and eccrine glands [3]. The effect of the sampling technique on the bacteria numbers yielded from the skin has been investigated; surface swabbing ~10,000 bacteria/cm^2, scraping of the *stratum corneum* ~50,000 bacteria/cm^2 and punches biopsies yielded ~1,000,000 bacteria/cm^2 [4]. The authors found that the number of bacteria increase with each additional dermatological layer sampled, supporting the earlier proposal of a 'hidden' flora [5]. These opportunistic pathogens found distributed throughout the skin *strata* can cause infection, particularly when the barrier is impaired, such as a surgical site incision [6]. For an antiseptic to neutralize the opportunistic skin pathogens found

residing below the superficial skin surface (7,8) the compound must permeate the skin barrier, the *stratum corneum* (9). The *stratum corneum* is the outer layer of the skin and is the rate-limiting barrier to the permeation of topically applied antibacterial compounds to the skin (10). The target of the antiseptic is below the superficial layers of the *stratum corneum*.

Chlorhexidine (1,6-di(4-chlorophenyl-diguanido)hexane) is a cationic bisbiguanide that has a broad spectrum of antimicrobial activity and has a low level toxicity to mammalian cells (11). It has been used throughout the global healthcare sector since it was first manufactured in 1954 by Rose and Swain (12). Commercially it is available in a range of formulations (water based, ethanolic, iso-propyl based) at varying concentrations (0.5–4%) (13). Chlorhexidine digluconate (CHG) is cationic at physiological pH which ensures that the biocide has a strong affinity for the negatively charged bacterial cell membrane. Chlorhexidine binds to the bacterial cell wall causing destabilization which results in leakage of the cytoplasmic contents, resulting in cell death.

While chlorhexidine has been used extensively in topical antimicrobial formulations, it has been shown in Franz cell diffusion studies to permeate into and across the skin poorly (9,14), leaving potential pathogens viable within the deeper layer of the skin. Chlorhexidine digluconate is water-soluble and is typically used in topical preparations. The physicochemical characteristics of chlorhexidine digluconate do not lend itself well for percutaneous permeation as it is in the ionized form (15) and has a molecular weight of 897.8 g/mol, which exceeds the optimal molecular weight for effective skin permeation (16). Furthermore, a log P (octanol/water) of 0.0133 is also less than optimal for effective percutaneous absorption (17).

In order to develop more efficacious strategies towards effective topical antisepsis it is imperative to first understand the localization and distribution of the antimicrobial compound throughout the skin *strata*, following its topical application, in order to determine whether the compound reaches the microbial reservoir. Mapping the location of a compound *in situ* within a biological tissue as complex as the skin, may also aid in elucidating the permeation pathway and mechanism of action. Conventional diffusion studies, such as those conducted using Franz-type skin diffusion cells, combined with tape stripping can yield informative dermatopharmacokinetic data (18,19) for topically applied drugs.

However, there is great inter-laboratory variability with regards to tape stripping methods and the methods are also laborious and time-consuming (20). There are also difficulties in standardizing the tape stripping to determine the amount of a compound in different layers of the epidermis due to the removal of varying amounts of the *stratum corneum*, inconsistent removal of skin layers (21). Whilst there have been advances in quantifying *stratum corneum* material on each tape strip, in a purely comparative sense, some are still laborious and time consuming. Gravimetric analysis (22)

and other methods require additional experimental techniques for example a modified protein Lowry assay (23). Other protein quantification techniques require further analytical equipment to that of the drug detection just for the detection of *stratum corneum* material such as a microscope (24), spectroscopic equipment (25) and infra-red densitometer (26). The ToF-SIMS technique allows many samples to be loaded on to the cryo-stage and consecutively analysed. There is no requirement for additional experiments to be conducted to quantify protein thus reducing the study time. ToF-SIMS not only has the ability to detect the drug or biomolecules of interest, it also has means of only including stratum corneum material in the analysis.

Imaging techniques that have been applied to mapping percutaneous absorption include confocal laser scanning microscopy (CLSM) (27), infra red (IR) imaging (28), confocal Raman microscopy (29), stimulated Raman scattering microscopy (30) and Matrix-assisted laser desorption/ionisation-time of flight mass spectrometry (MALDI-ToF) analysis. Confocal studies have the advantage of being able to capture 3D optical images of the skin but the information obtained is based upon a fluorophore, which may limit the application of the technique, particularly as species often require fluorescent "tagging". This restricts the number of compounds that can be analyzed by confocal microscopy; fluorescently tagging a compound may yield localization information within tissue that does not necessarily reflect that of the native compound. IR and Raman microscopes have an achievable spatial resolution (pixel size) of 6.25×6.25 µm and ~2 µm, respectively.

Recently, with the advent of stimulated Raman scattering microscopy, low sensitivity and interference signal from coherent nonresident background have been overcome, therefore it now offers label-free, non-invasive and real-time skin imaging (31). Stimulated Raman scattering microscopy is an exciting non-destructive skin imaging technique that has been used to image skin drug delivery of retinoic acid, the distribution of DMSO (31) and the chemical distribution of ibuprofen and ketoprofen throughout mammalian skin (30). Raman spectroscopy techniques offer the advantages of being a non-invasive three-dimensional high resolution imaging technique (32).

However, mass spectral imaging techniques offer unparalleled sensitivity. MALDI-ToF has been employed successfully to characterize the deposition of pharmaceutical compounds within skin but again lacks the desired spatial resolution (each pixel corresponds to 0.2 mm$^2 \times 0.2$ mm^2) (33). Within the Bunch *et al.* paper (33) the mass spectrum obtained had to be overlaid onto a haematoxylin and eosin stained skin section, which may be considered somewhat subjective. Whilst there is advanced MALDI software available to superimpose MALDI spectra over an optical image, it is not possible to distinguish morphological features only the tissue outline (34).

Therefore typically the tissue section would have to be histologically stained to correlate the tissue with the MALDI IMS spectra (35). There are nevertheless advancements being made and commercially available imaging MALDI instruments that have achieved a 20 μm spatial resolution when analyzing biological samples (36).

In order to achieve higher spatial resolution to map the distribution of a topically applied compound without the need for labeling or further skin processing the use of an alternative method, ToF-SIMS was explored. ToF-SIMS employs a cluster ion beam to raster primary ions onto the sample surface. A cascade collision occurs, resulting in the dissemination of secondary ions that are accelerated into the time-of-flight spectrometer. The advantages of ToF-SIMS include high mass resolution (>7,000), a large mass range (from the detection of elements up to the detection of molecular compounds), excellent spatial resolution (in the burst alignment mode) and an ability to simultaneously detect fragment ions over a large mass range that can be analysed retrospectively (37). ToF-SIMS mass spectra and retrospectively re-built chemical images not only highlight the localization of an exogenous compound within the tissue but can also profile the organic components of the different histological compartments of the tissue sample, allowing the depth of permeability to be estimated. Analysis can be undertaken in two modes: the bunched mode with high mass resolution and low spatial resolution, or the burst alignment mode (imaging mode), with high spatial resolution and low mass resolution.

Previous work using ToF-SIMS has investigated the incorporation of pseudo-ceramides in a cosmetic formulation within the *stratum corneum* (38,39). These studies used high resolution images of the skin surface to which the pseudo-ceramides had been introduced in order to demonstrate that synthetic pseudo-ceramides can effectively partition into the *stratum corneum*. This study also showed that the ToF-SIMS technique can provide valuable information regarding the distribution of cosmetic components within the skin. The application of ToF-SIMS to biomedical and biophysical applications has been shown previously. For example, photoageing effects on skin, before and after UV irradiation, were determined and changes in the ToF-SIMS maps of key skin components such as collagen and lipid molecules within a cross section of human skin were reported (40).

The primary aim of this study was to use ToF-SIMS to map the distribution and localization of a clinically relevant topical dose of chlorhexidine digluconate (2% w/v) once applied to dermatomed porcine skin. Furthermore, in order to validate the results, specifically with regards to the ingress of the chlorhexidine, a tape stripping study was undertaken in parallel using cryosectioned skin. These tape strips were also analysed by ToF-SIMS. It is our understanding that this is the first time ToF-SIMS has been utilised to visualize the distribution of a topical antiseptic applied to the skin.

MATERIALS AND METHODS

Chlorhexidine digluconate (CHG) 20% (w/v) and NaCl for physiological saline (0.9% w/w) were purchased from Sigma Aldrich, UK. Tape stripping was performed using adhesive tape purchased from Scotch tape, 3 M, UK. Analytical grade methanol, chloroform and hexane were obtained from Fisher, UK and were used to solvent clean glass cover-slips before sample mounting. De-gassed ultra pure water was used for the preparation of receptor fluid and for washings. Skin integrity was measured using Trans-Epithelial Electrical Resistance (TEER) LCR databridge, Tinsley, UK. Skin sectioning was conducted using a cryostat (Leica, CM1850). The temperature of the cryostat chamber was found to be optimal at −28°C. Samples were embedded within OCT embedding material, supplied by Fisher Scientific, UK. ToF-SIMS was performed using a ToF-SIMS IV instrument (IONTOF, GmbH, Münster, Germany) using a Bi_3^+ cluster source and a single-stage reflectron analyzer. ToF-SIMS data was analysed using IonTof software.

Skin Preparation

Pig skin was used within this study as it is regarded as the closest surrogate species for human skin in the field of percutaneous absorption. Pig flank skin has similar morphological properties and hair follicle density to man and using skin from pigs of the same age, sex and gene pool ensures that the model is homogenous. In contrast, abdominal skin for different human donors can vary with regard to penetration characteristics. Both pig and human skin are permitted as part of the human risk assessment process for cosmetic ingredients (41). On an ethical point, the pigs used in this investigation were specifically reared for food not for experimentation.

Skin was prepared from the flank of 6 week old pigs obtained from a local abattoir prior to any steam cleaning treatment. The skin was washed with distilled water and carefully shaved using clippers as to not damage the tissue. The subcutaneous fat was carefully removed using a scalpel and then the skin was dermatomed to a thickness of 400 μm with an electric dermatome. It was then wrapped in aluminum foil and frozen at −20°C until required. The dermatomed skin was then punched out with a 3 cm diameter punch and placed upon a stainless steel mesh support grid within a Franz diffusion cell, with the *stratum corneum* facing upwards. To check the integrity of the skin, 4.5 mL of physiological saline (0.9% w/w NaCl) was added to the receptor chamber and 2 mL of physiological saline was added to the donor chamber and placed in a circulating water bath on a submersible magnetic stirrer at 32°C for 30 min. After the cells had equilibrated, the TEER was measured to check the integrity of the porcine skin. Prior

to readings being taken, the instrument was calibrated using a resistor. It has been established that normal porcine skin in the Franz cells used should have an electrical resistance reading of ≥ 3 KΩ to pass the integrity check (42).

Diffusion (Franz-Type) Cell Study

The diffusion cells that had passed the integrity check were removed from the waterbath and the skin was allowed to air dry for 2 h at ambient temperature. 4.5 mL of physiological saline was added to the receptor chamber of each Franz cell. The Franz cells were placed in the water bath (32°C) on a submersible stirring plate for 30 min and allowed to equilibrate. A 2% (w/v) solution of CHG was prepared in distilled water from a 20% (w/v) solution of CHG. Once the Franz cells had equilibrated, an infinite dose (1 mL) of the CHG solution was applied to the skin surface and left for a contact time of 24 h. Excess CHG was removed from the skin surface of each diffusion cell by rinsing with 2 mL aliquots of distilled water (10 mL in total) over the surface of the dosed skin, taking care not to damage the skin. The skin was then allowed to air dry at ambient temperature, after which the Franz cells were dismantled and the skin destined for the cryosection experiment was snap frozen in liquid nitrogen. Each skin sample intended for the tape stripping work was stripped 21 times immediately after as described previously (43).

Sample Preparation for ToF-SIMS Analysis

The frozen skin samples were mounted on a cryostat using Optimal Cutting Temperature (OCT) embedding material. Vertical cross sections of skin of an 8 μm thickness were cut and placed on to a clean glass cover slip (1 cm × 1 cm). The cover slips were first rinsed in ultra-pure water followed by methanol and lastly chloroform, before the skin sample was loaded. For the tape strip experiment, 21 tape strips were taken to remove the *stratum corneum*. The strips were then freeze-dried and placed on a solvent-cleaned microscope slide ready for analysis.

ToF-SIMS Analysis

The cover slip containing the samples was mounted onto a cryo-stage with a cold finger mechanism and frozen to −80°C using a liquid nitrogen cooling system. The mounted skin samples were then exposed to an ultra high vacuum. A primary ion energy of 25 kV along with a pulsed target current of approximately 1 pA and post-acceleration energy of 10 kV were employed throughout the analysis. The primary ion dose density was maintained at less than 1×10^{12} ions per cm^2 throughout to ensure static conditions. Spectra were acquired in both the positive and negative mode at a resolution of 256 × 256 pixels by scanning a primary beam over the sample area.

Charge compensation of the sample was performed by irradiating the sample with a pulsed beam of electrons using an electron flood gun. Samples were analysed using both bunched and burst alignment modes thereby providing both high mass and spatial resolution data respectively. A reference sample of OCT was analysed whereby a small amount of the OCT embedding material was applied to a solvent cleaned cover slip. Data processing was performed using Surfacelab 6 for both spectroscopy and image analysis. Although data was collected in both positive and negative polarity, only the negative ion data will be presented as the positive ion data, though supportive, is much less informative. A scheme of the sample preparation and analysis can be observed in Fig. 1.

RESULTS AND DISCUSSION

Reference materials of OCT embedding material and a standard solution of CHG were analysed using ToF-SIMS in bunched mode (high mass resolution) revealing characteristic fragment ions. The following mass peaks were assigned as characteristic negative fragment ions corresponding to chlorhexidine digluconate: chlorine [m/z 35 and 37], $C_7H_4N_2Cl^-$ [m/z 151] and the chlorhexidine base parent molecular ion [m/z 505]. No secondary ion peaks corresponding to the OCT embedding material overlapped with the secondary ions characteristic of the CHG. Figure 2 shows a comparison of spectra a range of secondary ions that illustrate that the peaks are characteristic only of the CHG and are not inherent within the porcine tissue sections. The OCT embedding material and undosed control skin both show a low intensity secondary ion peak for chlorine as it is abundant within the natural tissue and environment. For this reason it would not act as a discriminatory peak for the compound of interest. The higher molecular weight fragment ion, $C_7H_4N_2Cl^-$ and the chlorhexidine molecular ion [m/z 505] are very distinctive and unique to CHG and this specificity is confirmed by their absence in the controls as shown in Fig. 2. The selected fragment ions are in abundance within the dosed tissue where a clear intensity peak is demonstrated in the mass spectrum of Fig. 2c.

It is possible to use the specific fragment ions to map the permeation of chlorhexidine into dosed porcine tissue. Figure 3 shows the distribution and localization of the fragment ions that are absent from the untreated skin. The chlorine [m/z 37] ion intensity for the 2% CHG treated skin sample is much higher and localized to the skin surface in contrast to the untreated sample. The chlorhexidine-treated sample has a higher ion intensity within the upper strata of the skin and there is a clear trend that with each skin sample illustrated the chlorine and the $C_7H_4N_2Cl^-$ ion [m/z 151] is strongly associated with the layers of the *stratum corneum*. The CHG characteristic ions are absent at a significant intensity
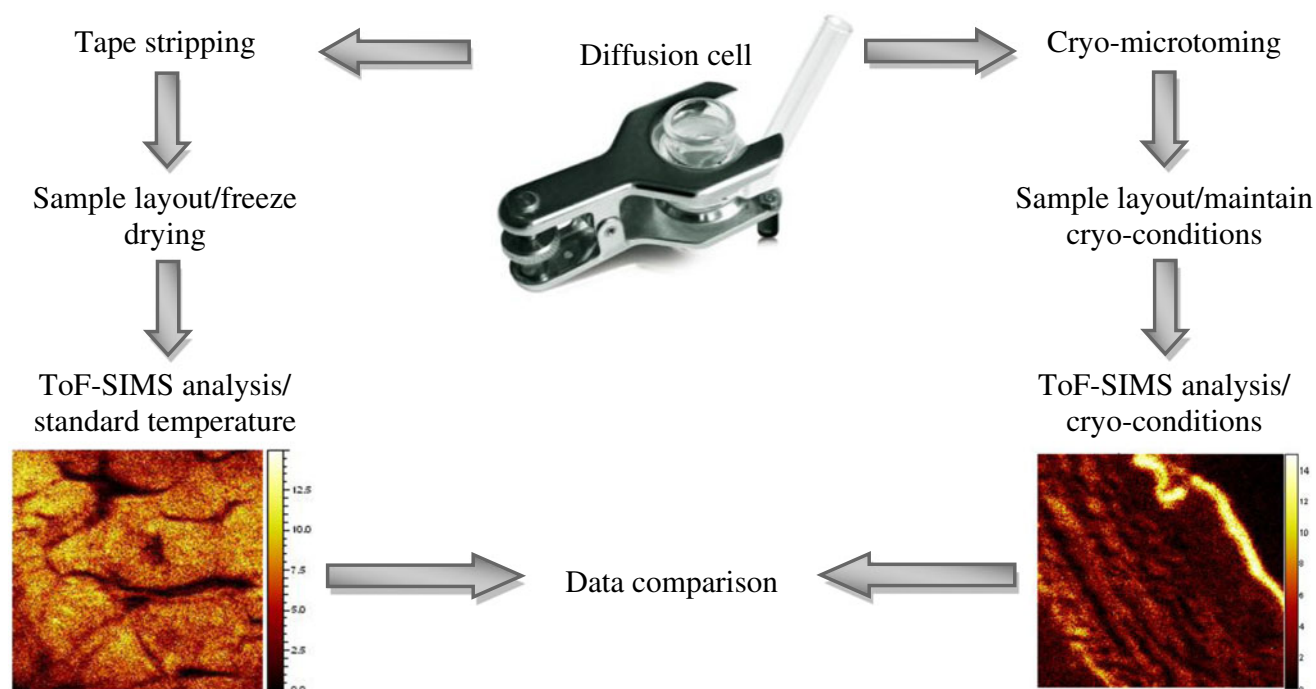
Fig. 1 Flow diagram illustrating the sample preparation and analysis.

within the deeper skin strata. The explicit localization trend of the ions characteristic of the CHG was observed repeatedly

with the CHG 2% (w/v) dosed porcine skin samples (Fig. 3). The chemical images obtained demonstrate the strong affinity
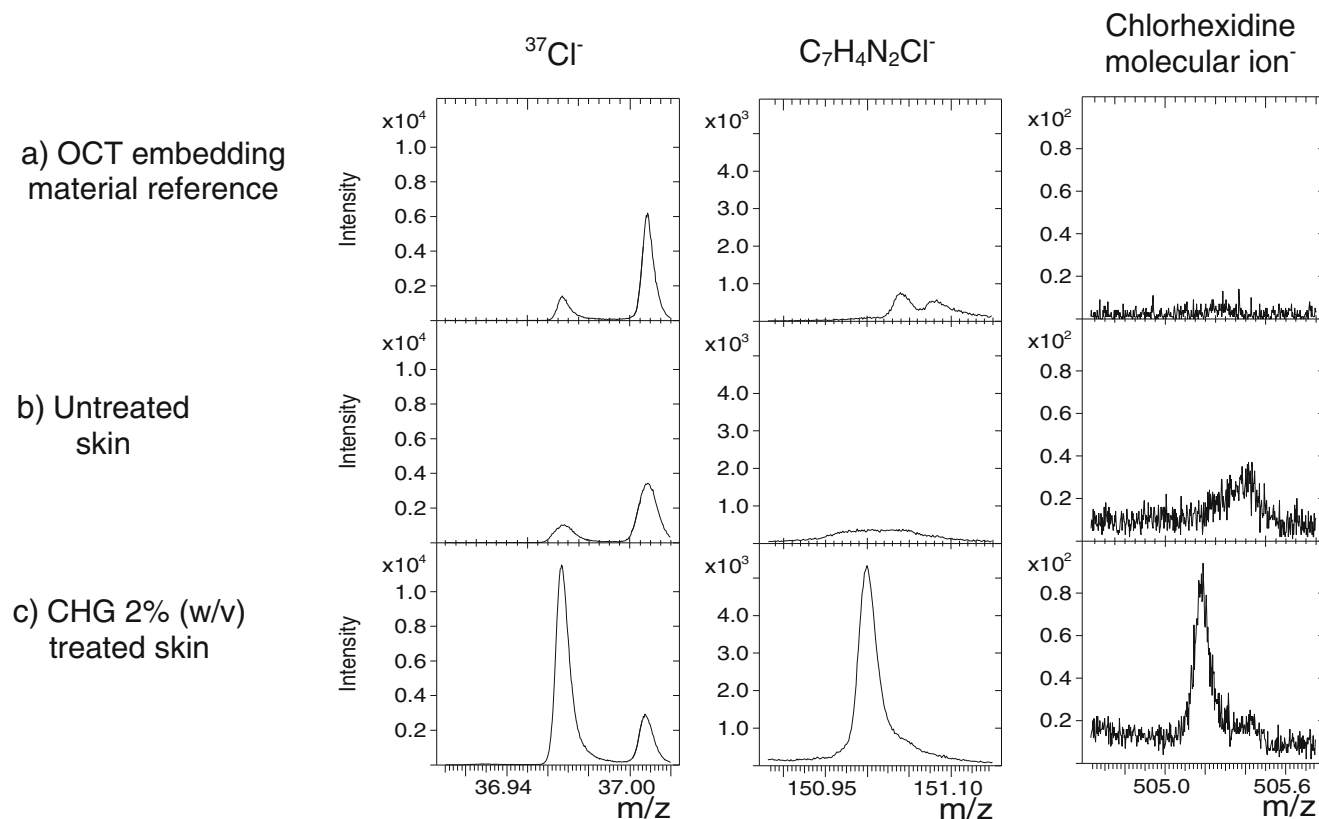

Fig. 2 ToF-SIMS mass spectra of various fragment ions ($^{37}Cl^-$, $C_7H_4N_2Cl^-$ and CHG base ion) present in OCT embedding material, untreated control skin and skin dosed with 2% CHG (w/v). The spectra were obtained in the negative ion mode.
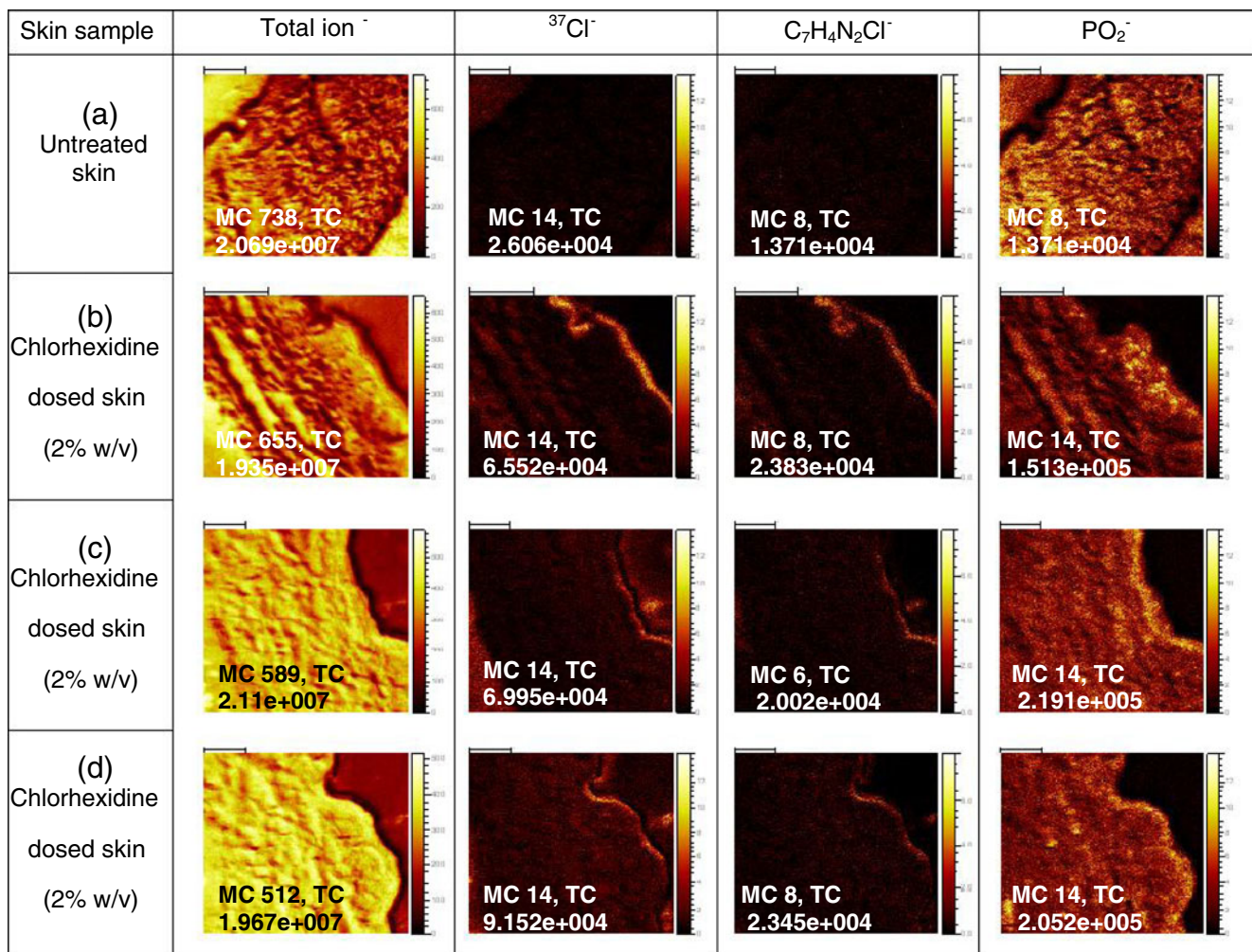
Skin sample	Total ion ⁻	³⁷Cl⁻	C₇H₄N₂Cl⁻	PO₂⁻
(a) Untreated skin	MC 738, TC 2.069e+007	MC 14, TC 2.606e+004	MC 8, TC 1.371e+004	MC 8, TC 1.371e+004
(b) Chlorhexidine dosed skin (2% w/v)	MC 655, TC 1.935e+007	MC 14, TC 6.552e+004	MC 8, TC 2.383e+004	MC 14, TC 1.513e+005
(c) Chlorhexidine dosed skin (2% w/v)	MC 589, TC 2.11e+007	MC 14, TC 6.995e+004	MC 6, TC 2.002e+004	MC 14, TC 2.191e+005
(d) Chlorhexidine dosed skin (2% w/v)	MC 512, TC 1.967e+007	MC 14, TC 9.152e+004	MC 8, TC 2.345e+004	MC 14, TC 2.052e+005

Fig. 3 ToF-SIMS images of various fragment ions of the negative control and 2% CHG (w/v) dosed porcine dermatomed skin (400 μm thick), where the scale bar represents 100 μm, *MC* maximum ion count per pixel and *TC* total ion count for the specific ion of interest.

that chlorhexidine has for the skin as it binds to the *stratum corneum* (44). The lack of CHG associated ions within the deeper skin *strata* illustrates the need for a permeation enhancement strategy in order to effectively neutralize bacteria found below the superficial layers of the *stratum corneum*.

ToF-SIMS has the capability to simultaneously map molecular ions associated with the applied compound and native fragment ions occurring within the tissue. A phosphate signal was also detected and mapped within the viable epidermis that was utilised to compartmentalize the tissue section into histological components; in this case, to identify the distinction between the viable epidermis and the *stratum corneum*. Phospholipids are not present in the *stratum corneum* due to the cornification process as free esterified sterols accumulate (45–47). This may aid the understanding of a dosed compound's localization within a complex tissue or highlight the presence of co-localization with native tissue molecules.

To further investigate the localization of CHG within the skin, the samples were analyzed using burst alignment mode (high spatial resolution). Although the overall mass resolution of the burst alignment mode spectra is reduced, each of the characteristic ions for CHG can still be resolved. High resolution chemical images of tissue samples were obtained and are shown in Fig. 4. Once the ions of interest are assigned in the high mass resolution spectra, the burst alignment mode can offer a wealth of spatial information. For example, Fig. 4 clearly shows the ³⁷Cl⁻ [*m/z* 37] attributed to the chlorinated aromatic ring of CHG tracking the *stratum corneum* and the chlorine is clearly observed at a relatively high intensity within the *stratum corneum* layers on the magnified burst-alignment image (Fig. 4).

To confirm the ingress of the CHG into the upper skin *strata*, a conventional tape-stripping experiment was conducted in parallel to the cryo-sectioning experiments. To remove the *stratum corneum*, 21 tape strips were taken from the dosed and washed skin samples. They were then
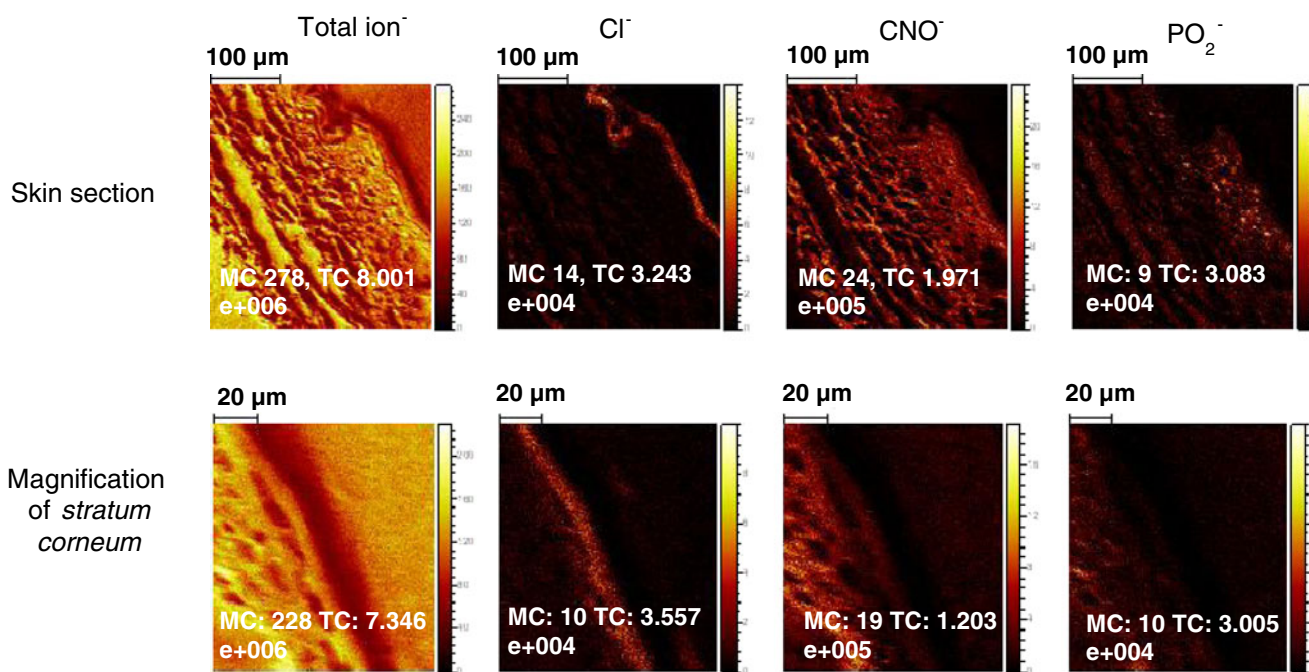
Total ion⁻   Cl⁻   CNO⁻   PO₂⁻

Fig. 4 ToF-SIMS images taken in burst alignment of various fragment ions liberated from the skin sample of 2% CHG (w/v) dosed porcine dermatomed skin (400 μm thick). The *stratum corneum* was magnified to enhance the visualisation of the ion distribution. *MC* maximum ion count per pixel and *TC* total ion count for the specific ion of interest.

freeze-dried and analysed using the method previously described ("Sample Preparation for ToF-SIMS Analysis"), to visualize the distribution of the characteristic CHG ions across the surface of the tape. Typically, beyond tape strip 5, it would be normal to pool the tape strips together (42) in order to achieve a concentration higher than the limit of
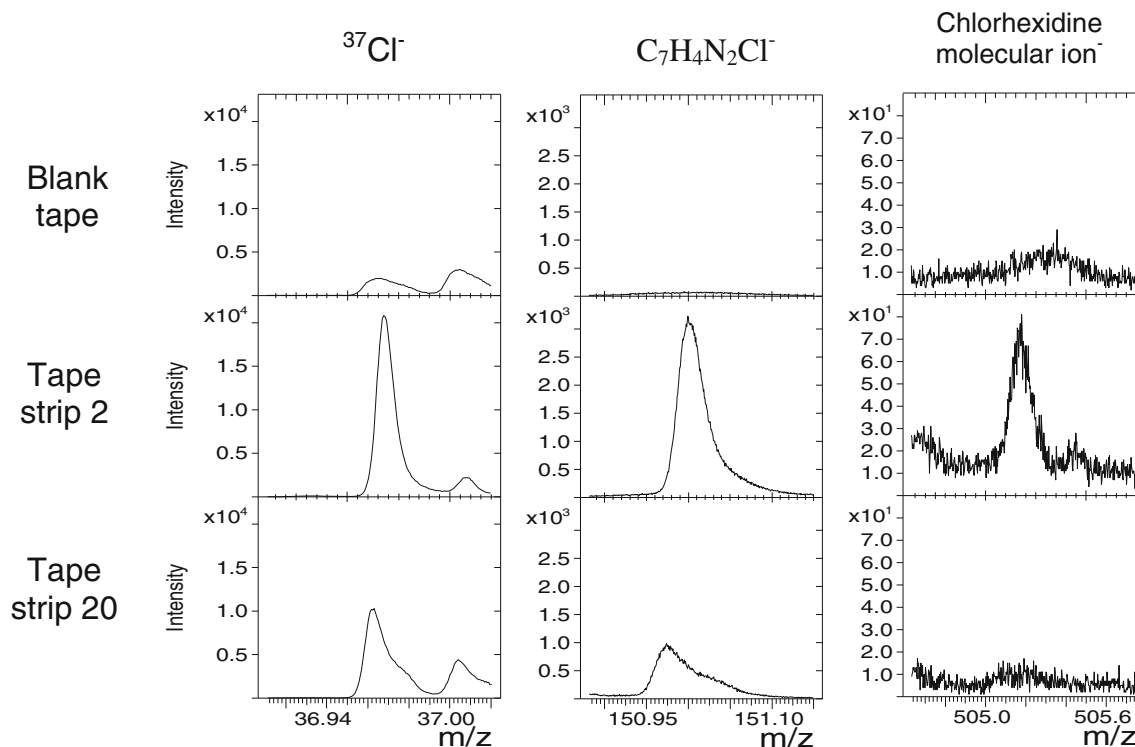

Fig. 5 ToF-SIMS mass spectra of various fragment ions (^{37}Cl$^-$, C$_7$H$_4$N$_2$Cl$^-$ and CHG base ion) present on the surface of control tape, tape strip 2 and tape strip 20 from skin dosed with 2% CHG (w/v). The spectra were obtained in the negative ion mode.
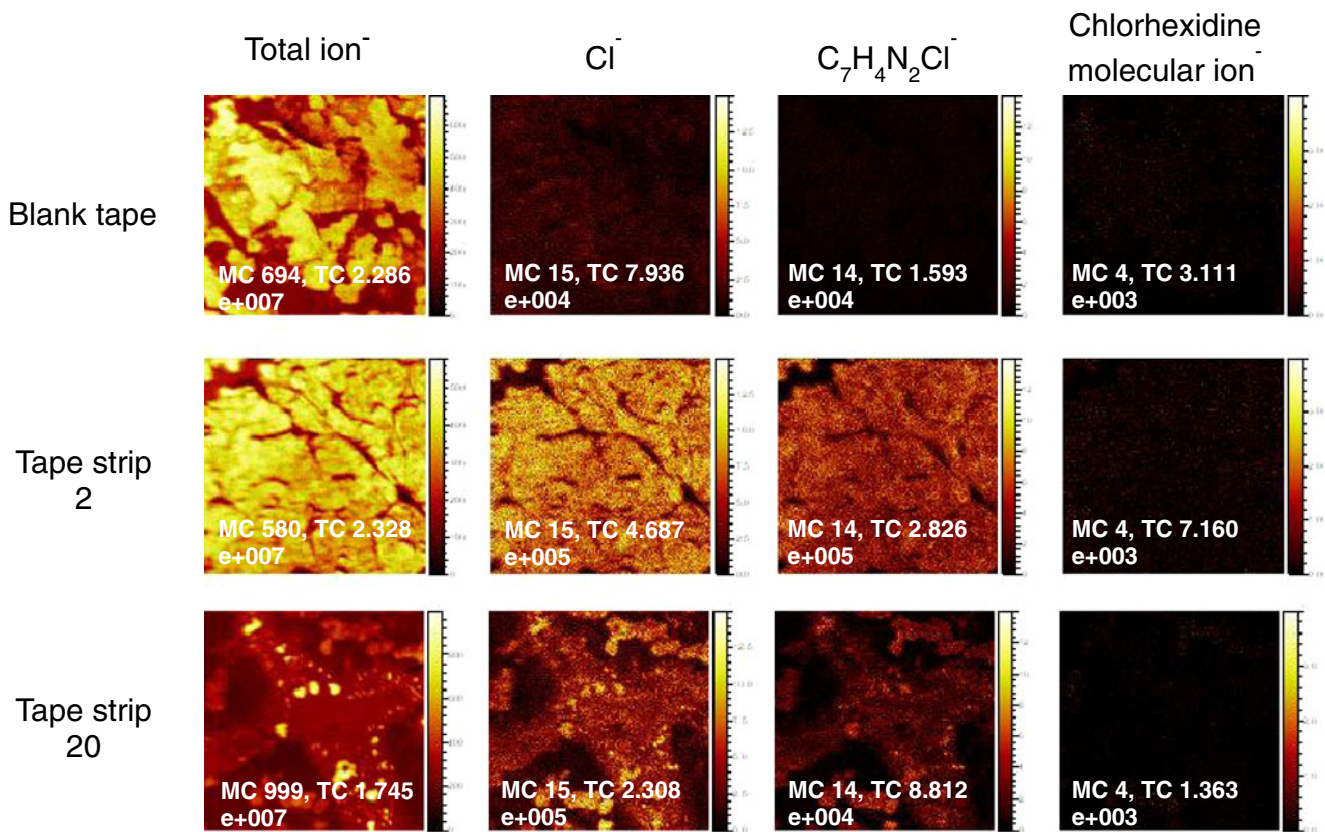
Fig. 6 ToF-SIMS images of various CHG specific ions of the negative control and representative tape strips 2 and 20 taken from 2% CHG (w/v) dosed porcine dermatomed skin (400 μm thick), *MC* maximum ion count per pixel and *TC* total ion count for the specific ion of interest.

detection (LOD) when using an analytical instrument such as high performance liquid chromatography (HPLC). The LOD for CHG extracted from skin section samples using a conventional HPLC assay was 0.016 μg/mL (9). The ppm sensitivity of the ToF-SIMS (37) circumvents this issue, where significant ion intensity can still be observed at tape strip 20 (Fig. 5).

A semi-quantitative depth profile of intensity of the compound's fragment ion of interest can be obtained by combining the tape stripping method with the ToF-SIMS analysis. A detailed explanation of the method development for this is illustrated elsewhere (48). Figure 6 illustrates the images obtained for the CHG associated negative fragment ions detected on the tape strips.

As the tape stripping progresses deeper into the *stratum corneum* a decreasing mass of material is removed from the sample, as observed in Fig. 6. A region of interest (ROI) can be selected i.e. only the *stratum corneum* material that can then be re-analysed after removing the background tape that contributes to the overall image and mass spectrum. The intensity of the compound fragment ion of interest within the selected ROI (*stratum corneum* material only) is normalized against the total ion intensity count for the selected ROI. The ability to analyse only the *stratum corneum* material can give a more accurate analysis of the drug deposition and

absorption throughout the layers of the *stratum corneum* and can thus confirm the substantivity of a compound within the superficial layers of the skin.

There was a decreasing trend observed for the CHG content on the region of interest on tape strips 1 to 21. The $C_7H_4N_2Cl^-$ [m/z 151] fragment ion generally decreases with the number of tape strips taken, with a small increase in ion intensity from tape strip 9 to 13. Tape strips 1 and 2 show a high concentration of $C_7H_4N_2Cl^-$ [m/z 151] that may correspond to adsorbed chlorhexidine that was not fully washed from the superficial layers of the *stratum corneum*. It is clear from the tape strip experiment (Figs. 5 and 6) that CHG is localized to the upper layers of the *stratum corneum* which is consistent with the results of the cryo-sectioned tissue results (Figs. 2 and 3). The strong association for the upper skin strata and poor permeation has also been observed elsewhere (14,15).

The ToF-SIMS data has shown that CHG applied to the skin surface as a 2% w/w solution binds to the upper layers of the *stratum corneum* and demonstrates poor permeation into the deeper tissues of the skin over the duration of the diffusion experiment. This lack of permeation may lead to an inefficient reduction in the microbial flora of the deeper skin strata (49), and also within the appendages such as the propionibacteria and staphylococcal bacteria found within

the hair follicles (50). This may suggest that the use of permeation enhancers, or the use of alternative topical antiseptic therapeutics, may be required in order to provide a more comprehensive reduction in the skin's micro flora, particularly below the *stratum corneum*.

CONCLUSION

This study has demonstrated that ToF-SIMS is capable of providing spatially relevant data for a topically applied compound once dosed onto porcine skin. Currently the method is only semi-quantitative, which is no different to a range of other skin visualization established techniques, including classical histology and spectroscopic methods. However, ToF-SIMS is a highly sensitive and powerful imaging technique which in this study has shown itself to be highly complementary to conventional Franz-type diffusion cell studies while in addition providing detailed profiles of permeation within the skin, particularly within the *stratum corneum*. This technique shows great promise for the characterisation of skin permeation and in the development of more efficient topical or transdermal formulations and compounds.

ACKNOWLEDGMENTS AND DISCLOSURES

REFERENCES

1. Eady E, Cove J. Staphylococcal resistance revisited: community-acquired methicillin resistant Staphylococcus aureus—an emerging problem for the management of skin and soft tissue infections. Curr Opin Infect Dis. 2003;16(2):103–24.

2. Great Britain. Health Protection Agency, Quaterly epidermiological commentary: mandatory MRSA, MSSA, E. coli bacteraemia and C. difficile infection data (up to October–December 2011). London, UK; 2003.

3. Roth R, James W. Microbial ecology of the skin. Annu Rev Microbiol. 1988;42:441–64.

4. Grice EA, Kong HH, Renaud G, Young AC, Bouffard GG, Blakesley RW, *et al*. A diversity profile of the human skin microbiota. Genome Res. 2008;18(7):1043–50.

5. Selwyn S, Ellis H. Skin bacteria and skin disinfection reconsidered. Br Med J. 1972;1(5793):136.

6. Paulson SD. Handbook of topical antimicrobials: Industrial applications in consumer products. London: CRC press; 2003.

7. Malcolm SA, Hughes TC. Demonstration of bacteria on and within the stratum corneum using scanning electron-microscopy. Br J Dermatol. 1980;102(3):267–75.

8. Hendley JO, Ashe KM. Eradication of resident bacteria of normal human skin by antimicrobial ointment. Antimicrob Agents Chemother. 2003;47(6):1988.

9. Karpanen TJ, Worthington T, Conway BR, Hilton AC, Elliott TSJ, Lambert PA. Penetration of chlorhexidine into human skin. Antimicrob Agents Chemother. 2008;52(10):3633–6.

10. Williams AC. Transdermal and topical drug delivery from theory to clinical practice. London: Pharmaceutical Press; 2003.

11. Denton WG. Chlorhexidine. In: Block SS, editor. Sterilisation and preservation. 5th ed. London: Lippincott Williams and Wilkins; 1991. p. 274–89.

12. Davies D, Ward R, Heylings J. Multi-species assessment of electrical resistance as a skin integrity marker for *in vitro* percutaneous absorption studies. Toxicol In Vitro. 2004;18(3):351–8.

13. Milstone AM, Passaretti CL, Perl TM. Chlorhexidine: expanding the armamentarium for infection control and prevention. Clin Infect Dis. 2008;46(2):274–81.

14. Lafforgue C, Carret L, Falson F, Reverdy M, Freney J. Percutaneous absorption of a chlorhexidine digluconate solution. Int J Pharm. 1997;147(2):243–6.

15. Smith J, Irwin W. Ionisation and the effect of absorption enhancers on transport of salicylic acid through silastic rubber and human skin. Int J Pharm. 2000;210(1–2):69–82.

16. Bos JD, Meinardi MMHM. The 500 Dalton rule for the skin penetration of chemical compounds and drugs. Exp Dermatol. 2000;9(3):165–9.

17. Farkas E, Kiss D, Zelko R. Study on the release of chlorhexidine base and salts from different liquid crystalline structures. Int J Pharm. 2007;340(1–2):71–5.

18. N'Dri-Stempfer B, Navidi WC, Guy RH, Bunge AL. Improved bioequivalence assessment of topical dermatological drug products using dermatopharmacokinetics. Pharm Res. 2009 Feb 2009;26(2):316–28.

19. Alberti I, Kalia YN, Naik A, Guy RH. Assessment and prediction of the cutaneous bioavailability of topical terbinafine, *in vivo*, in man. Pharm Res. 2001;18(10):1472–5.

20. Marttin E, Neelissen Subnel MTA, De Haan FHN, Bodde HE. A critical comparison of methods to quantify stratum corneum removed by tape stripping. Ski Pharmacol. 1996;9(1):69–77.

21. van der Molen RG, Spies F, vant Noordende JM, Boelsma E, Mommaas AM, Koerten HK. Tape stripping of human stratum corneum yields cell layers that originate from various depths because of furrows in the skin. Arch Dermatol Res. 1997;289(9):514–8.

22. Higo N, Naik A, Bommannan DB, Potts RO, Guy RH. Validation of reflectance infrared-spectroscopy as a quantitative method to measure percutaneous-absorption *in-vivo*. Pharm Res. 1993 Oct 1993;10(10):1500–6.

23. Dreher F, Modjtahedi BS, Modjtahedi SP, Maibach HI. Quantification of stratum corneum removal by adhesive tape stripping by total protein assay in 96-well microplates. Skin Res Technol. 2005 May 2005;11(2):97–101.

24. Lindemann U, Wilken K, Weigmann HJ, Schaefer H, Sterry W, Lademann J. Quantification of the horny layer using tape stripping and microscopic techniques. J Biomed Opt. 2003 Oct 2003;8(4):601–7.

25. Weigmann HJ, Lindemann U, Antoniou C, Tsikrikas GN, Stratigos AI, Katsambas A, *et al*. UV/VIS absorbance allows rapid, accurate, and reproducible mass determination of corneocytes removed by tape stripping. Skin Pharmacol Appl Skin Physiol. 2003 Jul–Aug 2003;16(4):217–27.

26. Voegeli R, Heiland J, Doppler S, Rawlings AV, Schreier T. Efficient and simple quantification of stratum corneum proteins on tape strippings by infrared densitometry. Skin Res Technol 2007 Aug 2007;13(3):242–51.

27. Alvarez-Roman R, Naik A, Kalia YN, Fessi H, Guy RH. Visualization of skin penetration using confocal laser scanning microscopy. Eur J Pharm Biopharm. 2004;58(2):301–16.

28. Mendelsohn R, Flach CR, Moore DJ. Determination of molecular conformation and permeation in skin via IR spectroscopy, microscopy, and imaging. Biochim Biophys Acta Biomembr. 2006;1758(7):923–33.

29. Zhang G, Moore DJ, Sloan KB, Flach CR, Mendelsohn R. Imaging the prodrug-to-drug transformation of a 5-fluorouracil derivative in skin by confocal Raman microscopy. J Invest Dermatol. 2007;127(5):1205–9.

30. Saar BG, Contreras-Rojas LR, Xie XS, Guy RH. Imaging drug delivery to skin with stimulated raman scattering microscopy. Mol Pharm. 2011 May–Jun 2011;8(3):969–75.

31. Freudiger CW, Min W, Saar BG, Lu S, Holtom GR, He C, et al. Label-free biomedical imaging with high sensitivity by stimulated raman scattering microscopy. Science. 2008;322:590–9.

32. Lademann J, Meinke MC, Schanzer S, Richter H, Darvin ME, Haag SF, et al. In vivo methods for the analysis of the penetration of topically applied substances in and through the skin barrier. Int J Cosmetic Sci. 2012;34(6):551–9.

33. Bunch J, Clench MR, Richards DS. Determination of pharmaceutical compounds in skin by imaging matrix-assisted laser desorption/ionisation mass spectrometry. Rapid Commun Mass Spectrom. 2004;18(24):3051–60.

34. Walch A, Rauser S, Deininger SO, Höfler H. MALDI imaging mass spectrometry for direct tissue analysis: a new frontier for molecular histology. Histochem Cell Biol. 2008;130(3):421–34.

35. Chaurand P, Norris JL, Cornett DS, Mobley JA, Caprioli RM. New developments in profiling and imaging of proteins from tissue sections by MALDI mass spectrometry. J Proteome Res. 2006;5(11):2889–900.

36. Lagarrigue M, Becker M, Lavigne R, Deininger SO, Walch A, Aubry F, et al. Revisiting rat spermatogenesis with MALDI imaging at 20-μm resolution. Mol Cell Proteomics. 2011 doi:10.1074/mcp.M110.005991.

37. Chabala JM, Soni KK, Li J, Gavrilov KL, Levisetti R. High-resolution chemical imaging with scanning ion probe sims. Int J Mass Spectrom Ion Process. 1995;143:191–212.

38. Okamoto M, Tanji N, Katayama Y, Okada J. TOF-SIMS investigation of the distribution of a cosmetic ingredient in the epidermis of the skin. Appl Surf Sci. 2006;252(19):6805–8.

39. Tanji N, Okamoto M, Katayama Y, Hosokawa M, Takahata N, Sano Y. Investigation of the cosmetic ingredient distribution in the stratum corneum using NanoSIMS imaging. Appl Surf Sci. 2008;255(4):1116–8.

40. Lee TG, Park J, Shon HK, Moon DW, Choi WW, Li K, et al. Biochemical imaging of tissues by SIMS for biomedical applications. Appl Surf Sci. 2008;255(4):1241–8.

41. SCCS, The Scientific Committee on Consumer Safety. Basic criteria for the in vitro assessment of dermal absorption of cosmetic ingredients. Updated, 2010; SCCS/1358/10.

42. Davies GE, Francis J, Martin AR, Rose FL, Swain G. 1:6-Di-4′-chlorophenyldiguanidohexane (hibitane); laboratory investigation of a new antibacterial agent of high potency. Br J Pharmacol Chemother. 1954;9(2):192–6.

43. Trebilcock KL, Heylings JR, Wilks MF. In-vitro tape stripping as a model for in-vivo skin stripping. Toxicol Vitr. 1994;8(4):665–7.

44. Aki H, Kawasaki Y. Thermodynamic clarification of interaction between antiseptic compounds and lipids consisting of stratum corneum. Thermochim Acta. 2004;416(1–2):113–9.

45. Elias PM. Stratum corneum defensive functions: an integrated view. J Invest Dermatol. 2005;125(2):183–200.

46. Lampe M, Burlingame A, Whitney J, Williams M, Brown B, Roitman E, et al. Human stratum corneum lipids: characterization and regional variations. J Lipid Res. 1983;24(2):120.

47. Reinertson PR, Wheatley VR. Studies on the chemical composition of human epidermal lipids. J Invest Dermatol. 1959;32:49–59.

48. Judd A, Scurr DJ, Heylings J, Wan KW, Griffiths D, Moss PG. Visualization of the permeation of chlorhexidine within the skin using Time-of-Flight Secondary Ion Mass Spectrometry (ToF-SIMS). In: Chilcott R, Brain KR, editors. Advances in dermatological science. London: Royal Society of Chemistry; 2013. In Press.

49. Brown E, Wenzel RP, Hendley JO. Exploration of the microbial anatomy of normal human skin by using plasmid profiles of coagulase-negative staphylococci: search for the reservoir of resident skin flora [with discussion]. J Infect Dis. 1989;160(4):644–50.

50. Touitou E, Meidan VM, Horwitz E. Methods for quantitative determination of drug localized in the skin. J Control Release. 1998;56(1–3):7–21.